Published in final edited form as:
Cell. 2010 March 5; 140(5): 704–716. doi:10.1016/j.cell.2010.01.026.

The Angelman Syndrome-associated ubiquitin ligase Ube3A regulates synapse development by ubiquitinating Arc

Paul L. Greer[1,2,6], **Rikinari Hanayama**[1,6], **Brenda L. Bloodgood**[1], **Alan R. Mardinly**[1], **David M. Lipton**[1], **Steven W. Flavell**[1], **Tae-Kyung Kim**[1], **Eric C. Griffith**[1], **Zachary Waldon**[5], **Rene Maehr**[4], **Hidde L. Ploegh**[4], **Shoaib Chowdhury**[3], **Paul F. Worley**[3], **Judith Steen**[5], and **Michael E. Greenberg**[1,*]

[1] Department of Neurobiology, Harvard Medical School, 220 Longwood Avenue, Boston, MA 02115

[2] Program in Biological and Biomedical Sciences, Harvard Medical School, 300 Longwood Avenue, Boston, MA 02115

[3] Department of Neuroscience, The Johns Hopkins University School of Medicine, Baltimore, MD 21205

[4] Whitehead Institute for Biomedical Research, Cambridge, MA 02142

[5] F.M. Kirby Neurobiology Center and Department of Neurology, Children's Hospital Boston, MA 02115

Abstract

Angelman Syndrome is a debilitating neurological disorder caused by mutation of the E3 ubiquitin ligase Ube3A, a gene whose mutation has also recently been associated with autism spectrum disorders (ASDs). The function of Ube3A during nervous system development, and how Ube3A mutations give rise to cognitive impairment in individuals with Angleman Syndrome and ASDs are not clear. We report here that experience-driven neuronal activity induces Ube3A transcription and that Ube3A then regulates excitatory synapse development by controlling the degradation of Arc, a synaptic protein that promotes the internalization of the AMPA sub-type of glutamate receptors. We find that disruption of Ube3A function in neurons leads to an increase in Arc expression and a concomitant decrease in the number of AMPA receptors at excitatory synapses. We propose that this deregulation of AMPA receptor expression at synapses may contribute to the cognitive dysfunction that occurs in Angelman Syndrome and possible other ASDs.

Introduction

Angelman Syndrome is a debilitating neurodevelopmental disorder that affects approximately 1:15,000 individuals and is characterized by motor dysfunction, severe mental retardation, speech impairment, frequent seizures, hyperactivity and a high prevalence of autism (Williams et al., 2006).Human genetic studies revealed that Angelman Syndrome (AS) is associated with *de novo* maternal deletions of chromosome 15q11-q13,

* To whom correspondence should be addressed: Tel: (617) 432-1772, Fax: (617) 734-7557, meg@hms.harvard.edu.
[6]Denotes co-first authors

paternal chromosome 15 uniparental disomy, or rare imprinting defects that affect the transcription of genes within 15q11-q13 (Clayton-Smith and Laan, 2003). More recent studies indicate that a failure to inherit a normal maternal copy of the *UBE3A* gene (which resides within 15q11-q13) accounts for 85-90% of all Angelman Syndrome cases. In this regard, specific loss-of-function mutations in the human *UBE3A* locus have been identified in a subset of affected individuals (Kishino et al., 1997; Matsuura et al., 1997).

The causative role of Ube3A mutations in AS is further supported by two independent mouse models generated by targeted inactivation of the *Ube3a* gene (Jiang et al., 1998; Miura et al., 2002). Upon inheritance of the mutation through the maternal but not the paternal germline, both mutant strains display several features of AS, including impaired motor function and seizures, as well as deficits in context-dependent and spatial learning. The finding that imprinting of the *Ube3A* gene occurs in specific brain regions, including the hippocampus, cerebellum, and regions of the neocortex, but not in non-nervous system tissues, reinforces the idea that the loss of Ube3A function in the central nervous system underlies AS pathology (Jiang et al., 1998; Albrecht et al., 1997;Yashiro et al., 2009).

The study of Ube3A mutations may also provide insight into the causes of autism. Autism spectrum disorders (ASDs) are complex neurological disorders characterized by an impairment in social interactions and the occurrence of repetitive behaviors. Despite the high prevalence of ASDs, very little is known about the cause or etiology of these cognitive disorders. Nonetheless, it is now appreciated that there is a significant genetic component to ASDs, and for this reason considerable effort has gone into identifying human genetic mutations that cause ASDs. These studies suggest that *Ube3A* is a candidate ASD gene. Genetic abnormalities within chromosomal region 15q11-q13 are among the most prevalent of all mutations identified in ASDs, accounting for approximately 1-2% of all ASD cases (Sutcliffe et al., 2003; Cook et al., 1997). Furthermore, recent reports indicate that copy number variance specifically within the *Ube3A* locus is associated with autism (Glessner et al., 2009). These data, together with the observation that individuals with Angelman Syndrome have a high prevalence of autism, suggest that mutation of Ube3A is likely to play a role in ASDs.

Despite the critical role that Ube3A plays in human cognitive function, relatively little is known about Ube3A's contribution to nervous system development or how the mutation of Ube3A leads to the cognitive impairment underlying Angelman Syndrome and ASDs. Electrophysiological experiments have demonstrated impaired long term potentiation (LTP) in the hippocampus of Ube3A knockout mice (Jiang et al., 1998). Additionally, a recent study implicates Ube3A in experience-dependent visual cortical plasticity (Yashiro et al., 2009). While these experiments demonstrate a crucial role for Ube3A in synaptic transmission and suggest that Angelman Syndrome may arise from a defect in synaptic function, the mechanisms by which Ube3A regulates synaptic function are poorly understood. Possible insight into how Ube3A functions may come from the finding that Ube3A is a member of the E3 ubiquitin ligase family of enzymes, a class of proteins that catalyzes the addition of ubiquitin moieties to target substrates, often leading to the degradation of the ubiquitinated protein. Genetic studies indicate that the ubiquitin ligase activity of Ube3A is necessary for normal human cognitive function inasmuch as the disruption of this activity leads to Angelman Syndrome (Cooper et al., 2004). Nevertheless, the neuronal substrates of Ube3A that mediate its effects on synaptic function remain unknown.

In this study we sought to understand how disruption of Ube3A results in synaptic dysfunction. We find that Ube3A is a neuronal activity-regulated protein that controls synaptic function by ubiquitinating and degrading the synaptic protein Arc. In the absence of

Ube3A, elevated levels of Arc accumulate in neurons resulting in the excessive internalization of AMPA receptors at synapses and impaired synaptic function. This impaired AMPA receptor trafficking may be a cause of the cognitive dysfunction that occurs in Angelman Syndrome. These findings suggest potential therapeutic targets for treating Angelman Syndrome, a disorder for which there is currently no effective therapy.

Results

Activity-dependent regulation of Ube3A

One clue as to how Ube3A might function in nervous system development comes from the observation that the symptoms of Angelman Syndrome and ASDs first become apparent within the first year or two of the child's life (Williams et al., 2006) a time during which sensory, motor, and cognitive experiences play a key role in shaping neuronal connectivity. The effect of environmental cues on cognitive development is manifested by the release of neurotransmitter at specific synapses which in turn triggers biochemical signaling events in the postsynaptic neuron, including a rapid and transient rise in the levels of intracellular calcium within the postsynaptic neuron. This increase in calcium drives synapse-specific changes including the insertion and removal of receptors from the plasma membrane, the translation or degradation of proteins localized to the synapse, and the post-translational modification of synaptic proteins. In addition, experience-driven neurotransmitter release initiates a program of gene expression that plays a critical role in synapse development and neuronal plasticity (Greer and Greenberg, 2008). A significant number of the components of the activity-dependent transcriptional program when mutated result in human neurological disorders (particularly ASDs and epilepsy) whose symptoms manifest in the first few years of human development. We therefore considered the possibility that Angelman Syndrome and a subset of ASDs may arise from a deficit in activity-dependent regulation of Ube3A.

We used quantitative real-time PCR to investigate the effect of neuronal activity on Ube3A expression. We found that the expression of Ube3A mRNA in cultured neurons is significantly increased by either membrane depolarization or glutamate receptor activation (Figure 1A). Conversely, blocking neuronal activity with APV to inhibit NMDA receptors, TTX to inhibit sodium channels, and NBQX to inhibit AMPA receptors results in a significant decrease in Ube3A mRNA expression (Figure S1A). We further found that Ube3A protein levels are reproducibly higher in neurons activated by membrane depolarization and significantly lower in neurons whose activity has been blocked (Figure 1B, S1B, and S1C).

We next asked if Ube3A expression is induced by neuronal activity in the intact mammalian brain. We found that during kainate-induced seizures, Ube3A mRNA and protein levels are significantly increased compared to control (Figure S1D and S1E). Ube3A is also induced in response to environmental stimuli that trigger experience-dependent synaptic development (Figure 1C and S1F). Mice were placed in a cage containing novel objects to induce exploratory behavior (enriched environment) as previously described (Nithianantharajah and Hannan, 2006) or were placed in a standard laboratory cage (control environment). Exposure to an enriched environment significantly increases Ube3A mRNA and protein expression (Figure 1C and S1F). Taken together, these results demonstrate that Ube3A mRNA and protein levels are regulated by synaptic activity both in culture and in the intact brain. These findings raise the possibility that early life experiences by triggering the release of glutamate at synapses activate Ube3A expression and that the absence of experience-dependent Ube3A induction may be a cause of the neurological impairment in Angelman Syndrome and autism spectrum disorders.

We next investigated the mechanism by which neuronal activity triggers Ube3A induction. Analysis of Ube3A transcripts present in EST databases revealed the existence of three distinct mRNA transcripts that are likely transcribed from three separate promoters. Of the three Ube3A transcripts, those initiating from promoters 1 and 3 are induced by neuronal activity (Figure S1G), and their promoters contain binding sites for the activity-regulated transcription factor MEF2. These sites are conserved across phylogeny, (including in human), and lie within 2kB of the putative transcriptional start sites of the two activity-regulated Ube3A transcripts (see below). The presence of potential MEF2-binding sites within Ube3A promoters was of interest because MEF2 has been previously shown to be an activity-regulated transcription factor that controls synapse development and regulates a number of genes that have been implicated in ASDs (Flavell et al., 2006; Flavell et al., 2008; Morrow et al., 2008).

To test if MEF2 binds to these conserved consensus binding sites in the Ube3A promoters, chromatin immunoprecipitation experiments were performed. DNA fragments that encompass Ube3A promoters 1 and 3 and include sequences that match the MEF2-binding site were enriched in anti-MEF2 immunprecipitates, but not in control immunoprecipitates (Figure 1D and data not shown). By contrast, there was no enrichment for DNA sequences surrounding Ube3A promoter 2, a region that lacks consensus MEF2 binding sites (Figure 1D). These data suggest that by binding to DNA sequences within Ube3A promoters 1 and 3, MEF2 may directly control the activity-dependent transcription of Ube3A.

Consistent with this possibility, we found that the neuronal activity-dependent induction of Ube3A promoter 1- and 3-driven mRNA transcripts and Ube3A protein are significantly reduced in neurons infected with lentiviruses encoding shRNAs that specifically target the MEF2 family members MEF2A and MEF2D, but are not affected by the presence of control shRNAs (Figure 1E, 1F, and S1G). By contrast, the expression of Ube3A promoter 2-dependent mRNA transcripts as well as GAPDH, beta3-tubulin, and CREM mRNAs are unaffected by the presence of MEF2 shRNA (Figure 1E and data not shown). Taken together, these experiments indicate that in response to neuronal activity, Ube3A promoter 1- and 3-driven mRNA transcripts and Ube3A protein expression are induced by a MEF2-dependent mechanism.

Identification of Ube3A substrates

The observation that Ube3A mRNA expression is regulated by neuronal activity, taken together with findings from human genetic studies implicating Ube3A in human neurobiological disorders such as Angelman Syndrome and ASDs, led us to investigate the role of Ube3A in nervous system development. Although little is known about Ube3A function in the nervous system, one important clue has come from human genetic studies. While the majority of Ube3A mutations that associate with Angelman Syndrome are either large chromosomal deletions, uniparental disomies, or nonsense mutations, a large number of point mutations within the Ube3A coding region have also been identified, nearly all of which abrogate the E3 ubiquitin ligase activity of Ube3A (Cooper et al., 2004). This observation suggests that the catalytic activity of Ube3A is critically important for nervous system development and that the identification of neuronal substrates of Ube3A might provide insight into how Ube3A regulates cognitive development.

Although several Ube3A substrates have been identified in non-neuronal cell types, the identification of substrates of E3 ubiquitin ligases has typically proved to be a daunting challenge due to 1) the absence of clear signature motifs within substrates of ubiquitin ligases 2) the transient nature of the ubiquitin modification as a consequence of the rapid turnover of ubiquitinated species, and 3) the low affinity of most ubiquitin ligases for their substrates (Scheffner et al., 1993; Kumar et al., 1999; Oda et al., 1999). We sought to

develop an approach for identifying substrates of E3 ligases which might circumvent these obstacles, employing a transgenic mouse in which a Hemagglutin epitope tagged-version of ubiquitin (HA-ubiquitin) is knocked into the HPRT locus (Ryu et al., 2007). These transgenic mice express similar levels of free ubiquitin in their brains to that detected in the brains of wild type mice (Figure 2A). In addition, in the HA-ubiquitin mice HA-ubiquitin appears to be efficiently incorporated into substrates (Figure 2A and B). We crossed HA-ubiquitin transgenic mice with wild type or Ube3A knockout mice and immunoprecipitated HA-ubiquitinated proteins from brain lysates of these mice. We then compared the entire complement of ubiquitinated proteins in wild type and Ube3A knockout mice using quantitative mass spectrometry. We reasoned that if a given protein were a substrate of Ube3A, then in the absence of Ube3A it would be significantly less ubiquitinated and thus less efficiently precipitated with anti-HA antibodies. We therefore sought to identify HA-ubiquitinated proteins whose abundance was decreased in Ube3A knockout mice.

Using this approach, we identified the protein Sacsin as a candidate Ube3A substrate. We found peptides corresponding to ubiquitinated Sacsin in brain lysates of wild type but not Ube3A knockout mice, suggesting that Sacsin might not be efficiently ubiquitinated in the absence of Ube3A (Figure 2C). Sacsin is of interest as it is mutated in the human disorder Charelvoix-Saguenay spastic ataxia, a neurological disorder with similarities to Angelman Syndrome, including ataxia, EEG abnormalities, lowered IQ, and some socialization deficiencies (Engert et al., 2000). However, little is known about Sacsin's role in nervous system development and the large size of the Sacsin protein suggested it would be difficult to study. Nevertheless, when we examined the amino acid sequence of Sacsin we found that Sacsin has a 60 amino acid stretch that has similarity to a previously identified Ube3A substrate HHR23A (Figure 2D). This region of homology corresponds to a well-characterized region of HHR23A consisting of five amphipathic helices suggesting that the corresponding region in Sacsin may have a similar structure (Kamionka and Feigon, 2004). As the specificity of ubiquitin ligases is most strongly determined by substrate binding, we hypothesized that this region of similarity between Sacsin and HHR23A might serve as a substrate recognition motif (hereafter referred to as Ube3A binding domain or UBD) for Ube3A that might facilitate the identification of additional Ube3A targets.

To begin to test this hypothesis, we generated a mutant form of HHR23A (ΔHHR23A) that lacks the UBD and assessed its ability to interact with, and be ubiquitinated by Ube3A. While wild type HHR23A efficiently interacts with Ube3A, mutation of the UBD in HHR23A blocks this interaction (Figure 2E). Likewise, this domain is required for Ube3A to ubiquitinate HHR23A (data not shown). Taken together, these results suggest the existence of a motif on Ube3A substrates that mediates binding to Ube3A.

A bioinformatics search of mammalian genomes for proteins that contain the Ube3A binding domain identified several proteins including the synaptic protein Arc and the RhoGEF ephexin 5 as potential Ube3A substrates (Figure 3A and Margolis et al., submitted). We focused our attention on Arc as Arc regulates the trafficking of alpha-amino-3-hydroxy-5-methyl-4-isoxazole-propionate (AMPA) type of glutamate receptors at synapses and thus if Arc is a substrate of Ube3A such a finding could potentially begin to explain Ube3A's role in synaptic function (Chowdhury et al., 2006; Rial Verde et al, 2006; Shepherd et al., 2006). Furthermore, like Ube3A, Arc transcription is regulated by neuronal activity through the action of MEF2 family transcription factors (Flavell et al., 2006). This coordinate regulation of Ube3A and Arc suggests that these two proteins might function together in response to synaptic activation.

To assess whether Arc is a Ube3A substrate, we first asked if Arc and Ube3A interact with each other. We found that purified recombinant Arc binds recombinant Ube3A in a manner

that is dependent upon the UBD within Arc (Figure 3B and 3C). Co-immunoprecipitation experiments using mouse brain extracts confirmed that Arc and Ube3A also interact in the intact brain (Figure S2A). To test if Arc is a substrate of Ube3A we performed *in vitro* ubiquitination assays using purified recombinant proteins. Recombinant Ube3A effectively ubiquitinated purified Arc *in vitro* but did not ubiquitinate the control proteins P53 or MeCP2 (Scheffner et al., 1993 (Figure 3D and data not shown)). Furthermore, a catalytically inactive form of Ube3A, (Ube3A C833A), was incapable of catalyzing the addition of ubiquitin moieties to Arc (Kumar et al., 1999) (data not shown and Figure 5A).

To test whether Ube3A promotes the ubiquitination of Arc within cells, we transfected HEK 293T cells with Arc and either Ube3A C833A or wild type Ube3A. Co-expression of wild type Ube3A, but not Ube3A C833A, led to a decrease in the level of Arc (Figure 3E). Incubation of transfected HEK293T cells with the proteasome inhibitor, MG132 blocked Ube3A-mediated degradation of Arc suggesting that Ube3A degrades Arc via the ubiquitin proteasome system (Figure S2B). The ubiquitination of Arc by Ube3A was confirmed by mass spectrometry which revealed that Ube3A catalyzed the polyubiquitination of Arc on Lysine 268 and 269 (Figures S2C and S2D).

To determine if Ube3A triggers the degradation of Arc in neurons, we compared Arc expression in the brains of wild type and Ube3A knockout mice. As the expression of both Ube3A and Arc is enhanced by neuronal activity, we exposed the mice to kainic acid or an enriched environment to boost the levels of Ube3A and Arc protein. Under these conditions, we detect higher levels of Arc protein in Ube3A knockout mice than in wild type controls (Figures 3F-3H). These findings suggest that Ube3A ubiquitination of Arc in the wild type brain contributes to Arc degradation. In contrast to Arc, the activity-dependent phosphorylation of the transcriptional regulator MeCP2, and the induction of the activity-regulated transcription factor NPAS4 are similar in wild type and Ube3A knockout brains suggesting that the increase in Arc levels in Ube3A knockout mouse brain is not the result of an overall increase in the activity-dependent gene response (Figure 3G and data not shown) (Zhou et al., 2006; Lin et al., 2008). Furthermore, Arc mRNA levels are similar in the brains of wild type and Ube3A knockout mice indicating that the increase in the level of Arc protein detected in Ube3A knockout neurons is likely due to a specific defect in Ube3A-mediated degradation of Arc rather than a change in the level of Arc mRNA (Figure 3I). Given that Arc is ubiquitinated by Ube3A *in vitro* and in intact cells, and the level of Arc protein is significantly higher in Ube3A knockout mice, we conclude that Arc is a *bona fide* Ube3A substrate and that the absence of Ube3A-dependent ubiquitination of Arc in Ube3A knockout mice results in increased levels of Arc in the brains of these animals.

Regulation of AMPA receptor expression and function by Ube3A

Arc regulates the surface expression of AMPA receptors (AMPARs), mediators of the majority of fast excitatory neurotransmission in the central nervous system. Reducing Arc expression leads to an increase in the surface expression of AMPARs, whereas increasing Arc levels decreases the plasma membrane expression of AMPARs (Chowdhury et al., 2006; Rial Verde et al, 2006; Shepherd et al., 2006). As Arc levels are significantly elevated in the absence of Ube3A, it is possible that there is a concomitant decrease in the expression of AMPARs on the plasma membrane. Such a finding would suggest a possible mechanism for the cognitive dysfunction observed in individuals with Angelman Syndrome.

We asked whether reducing Ube3A expression decreases the plasma membrane expression of AMPARs. We decreased Ube3A expression in hippocampal neurons by transfecting the neurons with shRNAs that specifically target Ube3A expression and then assessing the surface expression of AMPARs (Figure S3A and S3B). We focused our attention on the GluR1 subunit of the AMPA receptor as GluR1 insertion into the plasma membrane is

regulated by neuronal activity and by Arc (Newpher and Ehlers, 2008; Kessels and Malinow, 2009; Rial Verde et al, 2006; Shepherd et al., 2006). To examine GluR1 expression at the plasma membrane of neurons, we stained hippocampal neurons with anti-GluR1 antibodies under non-permeabilizing conditions and quantified the number of GluR1 puncta expressed on the cell surface. Expression of either of two shRNAs targeting Ube3A results in a marked reduction in the levels of GluR1 expressed at the plasma membrane and this reduction is rescued by co-expression of an RNAi-resistant form of Ube3A (Figure 4A and Figure S3C). This decrease in surface GluR1 was not due to a change in the synthesis or degradation of AMPARs as wild type and Ube3A-deficient cells expressed similar levels of GluR1 and GluR2 subunits (data not shown). Furthermore, the plasma membrane expression of NR1 subunits of the NMDA receptor was unaltered in Ube3A-deficient cells, suggesting that Ube3A selectively affects the cell surface expression of AMPARs (Figure 4B).

As AMPA receptors can also be trafficked in and out of synapses, we examined the effect of Ube3A knockdown on surface postsynaptic AMPA levels, quantifiying the number of GluR1 cell surface puncta that co-localize with the postsynaptic scaffolding protein PSD95. We find that shRNAs targeting Ube3A cause a significant reduction in the number of GluR1 puncta colocalizing with PSD95, indicating that Ube3A regulates recruitment of AMPA receptors to the postsynaptic region (Figure 4C).

We next asked if AMPAR endocytosis is enhanced in the absence of Ube3A. We used GluR1-specific antibodies to label surface AMPARs on neurons transfected with shRNAs targeted to Ube3A or scrambled controls. Following membrane depolarization to induce the endocytosis of synaptic AMPARs, anti-GluR1 antibodies bound to the remaining surface GluR1 subunits were removed by acid stripping (Man et al., 2007). Subsequent permeabilization of the cells and staining with fluorescently conjugated secondary antibodies to detect the internalized component of GluR1, revealed significantly increased levels of endocytosed GluR1 in Ube3A shRNA-expressing cells compared to control shRNA-transfected neurons (Figure 4D). Thus, the decreased expression of AMPARs in the plasma membrane of synapses of Ube3A-deficient cells is due, at least in part, to an increase in AMPAR endocytosis.

To investigate whether increased AMPAR endocytosis affects AMPAR function at synapses, we recorded miniature excitatory post synaptic currents (mEPSCs) in neurons expressing control or Ube3A-directed shRNAs. Compared to control shRNAs, the transfection of Ube3A shRNAs results in a significant decrease in mEPSC frequency with no significant change in mEPSC amplitude (Figure 4E, 4F, and 4G). This decrease in mEPSC frequency could be rescued by co-expression of an RNAi-resistant form of Ube3A. As mEPSC frequency is a measure of AMPA receptor-mediated synaptic transmission, this observation suggests that AMPA receptor function is altered at specific synapses of Ube3A deficient neurons.

The observation that when Ube3A expression is knocked down there is a reduction in mEPSC frequency with no change in mEPSC amplitude could be explained by any of three possibilities: 1) There could be a reduction in the number of synapses formed on the Ube3A deficient neuron, 2) there could be a reduced presynaptic probability of neurotransmitter release from neurons that synapse onto Ube3A deficient neurons, or 3) a subset of synapses that form on Ube3A deficient neurons could lack AMPA receptors and thus would be “silent synapses”, not readily detected by mEPSC recordings. To begin to distinguish between these possibilities, we first determined whether there are fewer synapses formed when Ube3A is knocked down. At the time point of analysis where we detect a clear reduction in AMPAR mEPSC frequency, we observe no significant change in either dendritic spine density or the number of synapses that form on Ube3A shRNA expressing neurons as detected by

immunohistochemical methods (Figure S3D and S3E). These findings, and the absence of any detectable change in the formation of inhibitory synapses, neuronal morphology, or cell survival associated when Ube3A expression is knocked down (data not shown), suggest that the decrease in mEPSC frequency does not reflect a decrease in the number of synaptic connections formed on Ube3A-deficient neurons.

Although we cannot formally rule out the possibility that a decrease in Ube3A expression in the post synaptic neuron reduces the presynaptic probability of release via a retrograde signal, we favor the hypothesis that the loss of Ube3A leads to the elimination of AMPA receptor expression from a subset of synapses for a number of reasons including: 1) we have found that the loss of Ube3A function results in an increase in the levels of Arc, a protein whose expression has been shown to promote the endocytosis of AMPA receptors, 2) in the absence of Ube3A we observe a decrease in the number of GluR1 puncta that colocalize with the postsynaptic marker PSD95 suggesting that when the level of Ube3A protein is reduced there are synapses that may not express AMPA receptors, 3) we find in additional experiments that there is a reduction in the ratio of AMPA/NMDA receptor-mediated transmission in Ube3A knockout neurons (see below) consistent with the idea that some of the synapses that form on Ube3A-deficient neurons lack AMPA receptors.

Arc mediates the effect of Ube3A on AMPA receptor trafficking

We next asked whether Ube3A enhances AMPAR endocytosis by ubiquitinating and degrading Arc. If the enhanced AMPAR endocytosis observed following Ube3A knockdown is mediated by the dysregulation of the ubiquitination and degradation of Arc, we would make the following predictions: 1) Ube3A's ubiquitin ligase activity would be required for its effect on AMPAR endocytosis. 2) The over-expression of Arc would phenocopy the loss of Ube3A and reduce AMPAR plasma membrane expression. 3) In Ube3A-deficient cells, restoring Arc expression to the level seen in wild type neurons should rescue the decrease in GluR1 surface expression observed in the absence of Ube3A.

To test these predictions, we first examined whether the ubiquitin ligase activity of Ube3A is required for Ube3A to promote AMPA receptor expression at synapses. We generated a Ube3A mutant in which the cysteine residue within the active site of the Ube3A ligase is mutated to an alanine (Ube3A C833A), reasoning that overexpression of this mutant should act in a dominant interfering manner by blocking the ability of endogenous Ube3A to ubiquitinate its substrates. We found this to be true as overexpression of Ube3A C833A specifically blocks the ability of wildtype Ube3A to ubiquitinate its substrates (Figure 5A, 5B, and 5C). To determine if Ube3A's ubiquitin ligase activity is required for Ube3A to enhance AMPAR expression at synapses, hippocampal neurons were transfected with wild type Ube3A or Ube3A C833A. Overexpression of Ube3A C833A but not wild type Ube3A, causes a significant reduction in the number of AMPARs present on the cell surface, suggesting that Ube3A ubiquitin ligase activity is critical to the ability of Ube3A to promote expression of AMPARs at synapses (Figure 5D and S4A).

We next asked whether the over-expression of Arc phenocopies the loss of Ube3A and reduces AMPAR expression. As previously reported, the over-expression of Arc results in a decrease in the plasma membrane expression of GluR1 (Chowdhury et al., 2006; Rial Verde et al, 2006; Shepherd et al., 2006 and Figure 5E). Co-expression of Ube3A with wild type Arc attenuates the ability of Arc to promote the endocytosis of GluR1 from the cell surface. When a version of Arc lacking the Ube3A binding domain (ArcΔUBD) was over-expressed in neurons, this form of Arc was still able to promote the endocytosis of GluR1 but the co-expression of Ube3A did not reverse this effect (Figure 5E). This suggests that Ube3A's ability to reduce the endocytosis of AMPARs is due to Ube3A-mediated degradation of Arc.

To further investigate the ability of Ube3A to promote the expression of AMPARs at synapses is due to Ube3A dependent Arc ubiquitination and degradation, hippocampal neurons were transfected with shRNAs targeting Ube3A to reduce Ube3A expression and/or shRNA directed against Arc to decrease Arc expression and the effect on AMPAR cell surface expression assessed. As described above, the expression of shRNAs targeting Ube3A in neurons led to a significant reduction in the number of AMPARs at the neuronal cell surface (Figure 5F). Introduction of shRNAs directed against Arc, but not control shRNAs, significantly reduced Arc expression in HEK293T cells (Figure S4B) and when transfected into neurons caused a small but statistically insignificant increase in surface AMPAR expression (Figure 5F). The failure of Arc shRNAs when transfected alone to significantly affect AMPA receptor surface expression likely reflects the fact that given the low level of neuronal activity in these cultures Arc levels are also quite low and only minimally affect AMPAR surface expression. Consistent with this possibility, in older cultures the expression of Arc shRNAs results in a significant increase in AMPAR plasma expression (Figure S4C). The lack of significant Arc expression in younger neuronal cultures may also explain why we find that over-expression of Ube3A does not significantly affect the plasma membrane expression of AMPARs in younger neuronal cultures. Expressing shRNAs against Ube3A together with an shRNA directed against Arc blocked the ability of Ube3A shRNA to suppress AMPAR expression at synapses (Figure 5F and S5). Taken together, these findings suggest that Ube3A promotes the expression of AMPARs at the plasma membrane of synapses by ubiquitinating and degrading Arc and that in the absence of Ube3A there is an excess of Arc protein, resulting in increased endocytosis of AMPARs.

Analysis of AMPA receptor function in Ube3A knockout mice

These findings suggest that in Angelman Syndrome the absence of Ube3A activity may lead to an increase in Arc expression, thereby resulting in a significant reduction in the expression and function of AMPARs at synapses. To begin to investigate this possibility, we examined AMPAR expression and function at the synapses of Ube3A knockout mice which display a number of features of Angelman Syndrome, including a high frequency of seizures, general ataxia, abnormal EEGs, and poor performance on tests of learning and memory and therefore serve as a useful animal model for Angelman Syndrome (Jiang et al., 1998). We cultured hippocampal neurons from Ube3A knockout mice and their wild type littermates and assessed the expression of AMPARs at the synapses of these neurons. We find that Ube3A knockout neurons have significantly reduced GluR1 expression at the plasma membrane of synapses when compared to wild type neurons (Figure 6A). This effect appears to be specific to AMPARs as we observe no change in the surface expression of NMDARs (Figure 6B). Consistent with our findings in Ube3A knockdown cells, we find that expression of shRNAs targeting Arc in Ube3A knockout neurons restores the expression of GluR1 surface expression in Ube3A knockout neurons (Figure 6C). These experiments suggest that the excessive internalization of AMPARs observed in Ube3A knockout neurons is likely a result of a failure to ubiquitinate and degrade Arc.

To determine if GluR1 expression at synapses is dysregulated in Ube3A knockout neurons in the context of an intact neuronal circuit, we employed array tomography, a technique in which ultra-thin sections of brain tissue are stained, imaged, and synapses visualized as a 3-D reconstruction (Micheva and Smith 2007). We performed array tomography using anti-GluR1 antibodies to visualize AMPARs and anti-SV2 antibodies to mark presynaptic sites and compared the stratum lucidum layer of CA3 of Ube3a knockout and wild type hippocampi. We find that the density of GluR1 puncta closely apposed to an SV2 puncta is decreased in Ube3a knockout mice (Figure 6D and S6). The density of SV2 puncta remained constant between the two genotypes, suggesting that the decrease in GluR1 synaptic

localization in Ube3A knockout sections is not a result of fewer available presynaptic sites and instead reflects a decrease in GluR1 expression at synapses. In contrast, we found that the number of NMDAR subunit NR1 puncta associated with SV2 puncta was similar at the synapses in the hippocampi of wild type and Ube3A knockout mice, suggesting that the expression of AMPARs is selectively decreased in the brains of Ube3A knockout mice (Figure 6E, 6F, and S6). This reduction in AMPAR expression at the synapses of Ube3A knockout mice is not a result of decreased overall expression of GluR1 as wild type and Ube3A knockout mice express similar levels of GluR1 and NR1 in their hippocampi (Figure 6G).

To determine if the decreased expression of AMPARs at the synapses of Ube3A knockout mice results in a functional decrease in synaptic transmission, acute hippocampal slices were prepared from wild type and Ube3A knockout mice, and AMPAR function was assessed by examining the ratio of AMPA/NMDA receptor-mediated currents by electrophysiological recordings. After minimal stimulation of Shaffer Collaterals, whole-cell recordings were made from CA1 pyramidal neurons to assess glutamate receptor function by measuring AMPAR- and NMDAR-mediated currents from a small group of synapses. We observe a significant decrease in the ratio of AMPA to NMDA receptor-mediated currents in Ube3A knockouts compared to wild type mice (Figure 7A and 7B). While this decrease in AMPA/NMDA receptor ratio could reflect either a decrease in AMPAR or an increase in NMDAR currents, our findings that in Ube3A knockout mice there is a decrease in AMPAR expression at synapses but no change in NMDAR expression suggests that the decrease in AMPA/NMDA current ratio is most likely due to a decrease in AMPAR-mediated currents in Ube3A knockout mice.

As an independent means of assessing the effect of disrupting Ube3A on AMPAR function, we recorded mEPSCs from wildtype and Ube3A knockout hippocampal pyramidal neurons in acute slice preparations. In accordance with our findings using shRNAs to reduce Ube3A expression, we observe a significant reduction in the frequency of mEPSCs with no corresponding change in mIPSC frequency or amplitude in Ube3A knockout neurons when compared to wild type neurons (Figure 7C- 7E and S7). As mEPSCs are a measure of AMPAR-mediated synaptic transmission, this observation supports the conclusion that AMPAR expression and function at synapses are significantly decreased in Ube3A knockout hippocampal neurons.

Discussion

Although it has been appreciated for more than a decade that mutation of Ube3A results in Angelman Syndrome, a debilitating human neurological disorder, remarkably little is understood about the role of Ube3A in nervous system development and function or why mutation of Ube3A results in the cognitive impairment underlying Angelman Syndrome. This lack of insight has greatly hampered the development of effective therapeutic strategies for treating Angelman Syndrome and as a result there are currently no effective treatments for this neurological disorder. In this study we demonstrate that in the absence of robust synaptic activation, Ube3A, as well as the synaptic protein Arc, are expressed at a low level. However, in response to glutamate release at excitatory synapses, Arc is induced with relatively rapid kinetics (Flavell et al., 2006) and functions to endoctyose AMPA receptors from the plasma membrane. This induction of Arc is likely important for limiting the level of neuronal excitation since the Arc-mediated endocytosis of AMPA receptors at synapses serves to dampen neuronal excitability. However, the level of Arc expression must be effectively regulated if synapses are to form and function appropriately. We find that Ube3A transcription is induced postsynaptically upon glutamate release at synapses with delayed kinetics relative to Arc and that Ube3A then functions to control the level of Arc protein

expression by ubiquitinating and degrading Arc. In this way Ube3A tempers the Arc-mediated internalization of AMPA receptors. The absence of Ube3A activity in Ube3A knockout mice results in increased levels of Arc expression, and consequently excessive internalization of AMPA receptors, leading to fewer synapses that express AMPA receptors at the plasma membrane and to defects in synaptic transmission.

Consistent with these observations, a recent study has demonstrated that Ube3A plays a critical role in experience-dependent synaptic plasticity (Yashiro et al., 2009). Although Ube3A was suggested to not be required for the initial sensory-independent stages of synapse development, Ube3A is necessary for sensory experience-driven maturation of excitatory circuits as Ube3A knockout mice have deficits in LTP, LTD, and decreased mEPSCs in visual cortex in response to visual experience. The observation that Ube3A selectively plays a role in experience-driven synaptic plasticity may be explained by our finding that both Arc and Ube3A transcription are induced by sensory experience-dependent neuronal activity and that in response to neuronal activity in the absence of Ube3A there is excessive accumulation of Arc and increased internalization of AMPARs. As AMPARs play a central role in neurotransmission and consequently information processing within the central nervous system, this defect in AMPAR expression and function in the absence of Ube3A is likely to explain, at least in part, the deficits in synaptic plasticity observed in the absence of Ube3A.

Our findings therefore suggest that Angelman Syndrome may be caused by the disruption of a crucial step in experience-dependent synaptic development, and provide evidence that the neuronal activity-regulated gene program plays a key role in human cognitive development. Further support for this hypothesis comes from the observation that mutation of another activity-regulated MEF2 target gene, Slc9A6, also results in phenotypes that closely mimic Angelman Syndrome (Gilfillan et al., 2008). Intriguingly, several recent studies have shown that additional components of the activity-regulated gene program including L-VSCC, RSK2, MeCP2, CBP, PDCH10, and DIA1 are mutated in human neurological disorders, particularly epilepsy and autism spectrum disorders (reviewed in Greer and Greenberg, 2008). Taken together, these findings suggest that further investigation into the regulation and function of Ube3A, and the activity-dependent gene program in general, will provide new insight into the mechanisms controlling human cognitive development, and how mutations that disrupt this process lead to developmental disabilities, including autism spectrum disorders.

The finding that disruption of Ube3A activity leads to a decrease in AMPAR expression at synapses suggests that drugs that promote an increase in the expression of AMPARs at synapses have the potential to reverse some of the symptoms associated with Angelman Syndrome. Studies of another human neurodevelopmental disorder Fragile X syndrome where a decrease in AMPAR expression at synapses has been observed suggest that this type of therapeutic strategy has potential. In Fragile X Syndrome, the observed decrease in AMPAR expression at synapses is due to excessive mGluR5 signaling resulting in increased Arc translation and consequently excessive AMPAR internalization (Dolen and Bear, 2008). In a mouse model of Fragile X Syndrome injection of the mGluR5 antagonist MPEP restored surface expression of AMPARs and prevented the symptoms associated with Fragile X Syndrome (Dolen et al., 2007; Nakamoto et al., 2007; Yan et al., 2005). These results have led to the development of more specific mGluR5 antagonists that are now entering clinical trial for the treatment of Fragile X syndrome. It is possible that similar approaches will also be effective for treating Angelman Syndrome.

A recent study demonstrated that the mutation of an inhibitory phosphorylation site of alphaCaMKII rescues many of the behavioral deficits exhibited by Ube3A-deficient mice

suggesting that subtle genetic manipulations may be sufficient to reverse Ube3A loss-of-function phenotypes (van Woerden et al., 2007). An intriguing aspect of this finding is that increasing CamKII activity (by blocking inhibitory phosphorylation) results in an increase in AMPARs expressed at synapses (Rose et al., 2009) and this may explain why mutating the inhibitory phosphorylation site of CaMKII is able to rescue the phenotypes associated with the loss of Ube3A.

Although our results provide hope that it will be possible to develop therapies for treating individuals with Angelman Syndrome, it is also likely that the defect in AMPAR expression at synapses is not the only thing that has gone awry in Angelman Syndrome. For example, it is not obvious how impaired AMPAR receptor function results in an increased susceptibility to seizures and thus it is likely that Ube3A substrates in addition to Arc play roles in nervous system development. In addition to increased susceptibility to seizures, individuals with Angelman Syndrome also have sleep disturbances, hyperactivity, inappropriate laughter and movement disorders. Given the broad phenotypic consequences of Angelman Syndrome, it seems likely that the disruption of the degradation of a number of Ube3A substrates contributes to Angelman Syndrome pathology. In the present study, we have defined a Ube3A binding motif which has aided in the identification of new Ube3A substrates. One of these Ube3A substrates is the RhoGEF ephexin5 which plays an important role in restricting the number of synapses formed by a neuron (Margolis et al., submitted). We have also identified Sacsin as a Ube3A substrate which is mutated in the human neurodevelopmental disorder Charlevoix-Saguenay spastic ataxia and it is intriguing to speculate that in Angelman Syndrome, the absence of Ube3A-mediated ubiquitination of Sacsin may contribute to the movement disorders associated with Angelman Syndrome. In addition to ephexin5 and Sacsin, we have identified a number of other proteins which contain the Ube3A binding motif. It will be important in the future to determine how these substrates work together with Ube3A to fine tune synapse development and cognitive function.

Experimental Procedures

Cell cultures, transfections, and infections

HEK293T cells and hippocampal neurons were cultured, transfected, and infected as previously described (Flavell et al., 2006). Organotypic slice cultures were prepared from P3-6 rat or mouse brains and 350 μm slices of hippocampus were prepared and transfected as described previously (Zhou et al., 2006). Acute slices were prepared from P15-18 mice as described previously (Lin et al., 2008).

Mice

Ube3A knockout mice were obtained from The Jackson Laboratory, strain 129-*Ube3a*^{tm1Alb}/J from stock number 004477. HA-ubiquitin mice were previously described (Ryu et al., 2007). Seizures were induced for three hours in adult CD1 mice by intraperitoneal injection of kainic acid (Ocean Produce International) at a dose of 25 mg/Kg. For enriched environment experiments, 6 week old CD1 male mice were either placed in standard laboratory cages or in cages containing a variety of rodent toys of various shapes and colors (PETCO) for three hours.

Quantitative Real-Time PCR

Total RNA was harvested from hippocampal neurons at 10 DIV following stimulation with the indicated agent using the RNeasy mini kit (Qiagen). Stimulants included Bicuculline (Sigma, 20 μm), Glutamate (Sigma, 10 μm), NMDA (Sigma, 20 μm), recombinant human BDNF (Peprotech, 50 ng/mL), NT3 (Peprotech, 50 ng/mL), NT4 (Peprotech, 50 ng/mL), and 55 mM KCl as previously described (Chen et al., 2003). Reverse transcription was

performed using SuperScript III (Qiagen), and quantitative RT-PCR using SYBR Green Master Mix was performed on an ABI Prism 7700 according to the manufacturer's instructions. The primers used for this study are listed below:

ArcF: 5′-ACCGTCCCCTCCTCTCTTGA-3′;

ArcR: 5′-TCTTTGTAATCCTATTTTCTCTGCCTT-3′

Beta3-tubulinF: 5′-CCCGAGGGCTCAAGATGTC-3′

Beta3-tubulinR: 5′-TCTTTGTAATCCTATTTTCTCTGCCTT-3′

CremF: 5′-AAAGCGGGAGCTGAGGCT-3′

CremR: 5′-TTCTTTCTTCTTCCTGCGACACT-3′

GapdhF: 5′-TCCATGACAACTTTGGCATCGTGG-3′

GaphdhR: 5′-GTTTCTGTTGAAGTCACAGGAGAC-3′

Ube3aF: 5′-TCCTCTTTGGGTGACTCCAG-3′

Ube3aR: 5′-CGGAAGAGAAGCGTAACGAG-3′

Chromatin Immunoprecipitation

Chromatin immunoprecipitation was performed using the ChIP assay kit (Upstate) as previously described (Flavell et al., 2006). The consensus binding site for MEF2 is C/TTAWWWWTAA/G. Primers used for these assays are listed below:

Ube3A promoter 1 F: 5′-GCTCTGGTGGGGAAGACATA -3′

R: 5′-CCAGAAGCAGCACACGAATA-3′

Ube3A promoter 2 F: 5′-AGAAACCTCATAGTGCTTGCAG-3′

R: 5′-TTCTCAACTCTGGCCATCAA-3′

Ube3A promoter 3 F: 5′-TCTGCCCTCTCTACGTCAGG-3′

R: 5′-ATGAAACGAAACCCCACAAG-3′

Image Analysis

Images were acquired on a Zeiss LSM5 Pascal confocal microscope. For spine and synapse analysis, 12-bit images were acquired with a 63× objective at 1024×1024 pixel resolution. Images were acquired using z-stacks of 0.48 μm thickness. Maximum intensity projections were created from the z-stacks and analyzed using MetaMorph image analysis software (Molecular Devices). For each experiment image acquisition and image analysis were performed blinded to genotype and/or condition. Quantification of dendritic spine densities, lengths and widths were obtained manually using MetaMorph software. For all spine measurements at least 200 μm of dendrite was used for each neuron.

Plasmids

pSuper plasmids targeting MEF2A and MEF2D were previously described (Flavell et al., 2006). Bacterial and mammalian expression plasmids of wild type Ube3A were generously provided by P. M. Howley (Kumar et al., 1999). QuikChange mutagenesis was used to generate Ube3A C833A. Bacterial and mammalian expression plasmids for Arc were previously described (Chowdhury et al., 2006). Arc and Ube3A shRNAs were generated using the pSuper RNAi system (OliogoEngine, Seattle, WA) and the following sequences: Ube3A RNAi #1: 5′-TC**T**CC**A**C**A**G**T**CC**T**GA**AT**AT-3′, Ube3A RNAi #2 5′-CCC**AAT**GA**T**G**T**ATG**A**TCT**A**-3′, Arc RNAi #1 5′AC**C**C**A**A**T**GTGAT**C**CTGCAG-3′, Arc

RNAi #2 5′-GC**T**G**AT**GGC**TA**CG**A**C**TA**C**A**-3′ (mismatches listed in bold for scrambled constructs). The following sequences were used to generate RNAi-resistant forms: Ube3Ares #1: TCTGCATAGCCCGGAGTACCTG, Ube3ares#2: TCCGATGATGTACGACCTGAAG, Arcres#1: ACCGAACGTCATACTCCAA, Arc Res#2: GCGGACGGGTATGATTATA.

Ubiquitination Assay and *in vitro* binding

2 μg of Arc C-terminal protein (132-396 a.a.) was incubated with 2 μg of GST-WT or mutant Ube3A (C833A) in binding buffer (20 mM Tris-HCL, pH 7.4, 50 mM NaCl, 4 mM ATP, 10 mM MgCl2, 0.2 mM dithiothreitol and 1% Triton X-100). After 2 h of mixing at 4°C, glutathione-Sepharose beads (GE Healthcare) were added and incubated for another 2 h. The beads were washed twice with PBS + 1% Triton X-100 and twice with PBS. Proteins were eluted with SDS sample buffer and analyzed by Western blotting. For in vitro ubiquitination assays, 1 μg of Arc C-terminal protein was incubated with 50 ng of E1, 100 ng of UbcH7, 200 ng each of WT or mutant (C833A) Ube3A, and 4 μg of ubiquitin (BostonBiochem) in 20 mM Tris-HCL, pH 7.4, 50 mM NaCl, 4 mM ATP, 10 mM $MgCl_2$, and 0.2 mM dithiothreitol. Reactions were terminated after 2 h at 30 °C by the addition of SDS sample buffer and were analyzed by Western blotting.

Surface GluR1 staining

Immunostaining of surface GluR1 receptors was performed as previously described (Chowdhury et al., 2006).

Electrophysiology

Electrophysiology was performed using standard methods (see supplemental information for more detail).

Ube3A knockout cultures

Hippocampal cultures were prepared from Ube3A knockout and wild type littermate mice at P2 using a protocol adopted from K. Condon and M. Ehlers. Briefly, hippocampi were dissected in Dissociation Media (DM) (0.3% BSA, 12 mM MgSO4, 10 mM HEPES, 0.6% glucose in Hanks Balanced Salt Solution). Hippocampi were then placed in a papain solution 30 Units/mL in DM for fifteen minutes before resuspending in Neurobasal Medium. The cells were then plated on glass coverslips which had been coated overnight with PDL.

Array Tomography

Array tomography was performed as described (Micheva and Smith, 2007). In summary, acute hippocampal slices (300 um thick) were fixed in 4% paraformaldyhde for 1 hour at room temperature and embedded in LR White resin using the benchtop protocol. Ribbons of between 30-50 serial 100 nm sections of both WT and Ube3a KO were mounted side by side on subbed glass coverslips. Coverslips were immunostained with anti-SV2 (ms, DSHB, 1:100) and anti-GluR1 (Rb, Millipore, AB1504) or anti-NR1 (Rb, Millipore AB9864, 1:100) antibodies as described. Serial sections were imaged using a Zeiss Imager.Z1 microscope with a Photometrics CoolSNAP HQ2 camera on a PLAN APO 63×/1.4 objective. Tissue volumes were aligned using ImageJ (NIH) with the multistackreg plugin (Brad Busse). Reconstructed tissue volumes were cropped to include only stratum lucidum of CA3 and analyzed in Bitplane Imaris and custom software to count synapses. A synapse was counted if the distance between the center point of an SV2 puncta and a GluR1/NR1 puncta was equal to or less than the sum of the radii of the two puncta plus an empirically determined scaling factor of .15 μm. All experiments were carried out and analyzed blinded to genotype.

Supplementary Material

Refer to Web version on PubMed Central for supplementary material.

Acknowledgments

We thank members of the Greenberg lab for helpful suggestions. In particular, we would like to thank S. Margolis for sharing unpublished results and C. Chen, J. Zieg and S. Cohen for helpful discussions and critical reading of this manuscript; J. Zieg for assistance with figure making, S. Vasquez for preparation of primary neuronal cell cultures; Drs. K. Condon and M. Ehlers for their generous advice on culturing Ube3A knockout neurons; E. Bennechi for sectioning array tomography ribbons. This research was supported by a National Science Foundation predoctoral fellowship (P.L.G), a Human Frontier Science Program Fellowship (R. H.), a grant from NIMH (MH53608 to P.F.W), and an Angelman Syndrome Foundation grant during the initial stages of this work, and NIH grant (NS28829) (M.E.G).

References

Albrecht U, Sutcliffe JS, Cattanach BM, Beechey CV, Armstrong D, Eichele G, Beaudet AL. Imprinted expression of the murine Angelman syndrome gene, Ube3A, in hippocampal and Purkinje neurons. Nat Genet 1997;17:75–78. [PubMed: 9288101]

Chen WG, Chang Q, Lin Y, Messner A, West AE, Griffith EC, Jaenisch R, Greenberg ME. Derepression of BDNF transcription involves calcium-dependent phosphorylation of MeCP2. Science 2003;302:885–889. [PubMed: 14593183]

Chowdhury S, Shepherd JD, Okuno H, Lyford G, Petralia RS, Plath N, Kuhl D, Huganir RL, Worley PF. Arc/Arg3.1 interacts with the endocytic machinery to regulate AMPA receptor trafficking. Neuron 2006;52:445–459. [PubMed: 17088211]

Clayton-Smith J, Laan L. Angelman Syndrome: a review of the clinical and genetic aspects. J Med Genet 2003;40:87–95. [PubMed: 12566516]

Cook EH, Lindgren V, Leventhal BL, Courchesne R, Lincoln A, Shulman C, Lord C, Courchesne E. Autism or atypical autism in maternally but not paternally derived proximal 15q duplication. Am J Hum Genet 1997;60:928–934. [PubMed: 9106540]

Cooper EM, Hudson AW, Amos J, Wagstaff J, Howley PM. Biochemical analysis of Angelman Syndrome-associated mutations in the E3 ubiquitin ligase E6-associated protein. J Biol Chem 2004;279:41208–41217. [PubMed: 15263005]

Dolen G, Osterweil E, Rao BS, Smith GB, Auerbach BD, Chattarji S, Bear MF. Neuron 2007;56:955–962. [PubMed: 18093519]

Dolen G, Bear MF. Role for metabotropic glutamate receptor 5 (mGluR5) in the pathogenesis of fragile X syndrome. J Physiol 2008;586:1503–1508. [PubMed: 18202092]

Engert JC, Berube P, Mercier J, Dore C, Lepage P, Ge B, Bouchard JP, Mathieu J, Melancon SB, Schalling M, Lander ES, Morgan K, Hudson TJ, Richter A. ARSACS, a spastic ataxia common in northeastern Quebecv, is caused by mutations in a new gene encoding an 11.5-kb ORF. Nat Genet 2000;24:120–125. [PubMed: 10655055]

Flavell SW, Cowan CW, Kim TK, Greer PL, Lin Y, Paradis S, Griffith E, Hu LS, Chen C, Greenberg ME. Activity-dependent regulation of MEF2 transcription factors suppresses excitatory synapse number. Science 2006;311:1008–1012. [PubMed: 16484497]

Flavell SW, Kim TK, Gray JM, Harmin DA, Hemberg M, Hong EJ, Markenscoff-Papadimitrious E, Bear DM, Greenberg ME. Genome-wide analysis of MEF2 transcriptional program reveals synaptic target genes and neuronal activity-dependent polyadenylation site selection. Neuron 2008;60:1022–1038. [PubMed: 19109909]

Gilfillan GD, Selmer KK, Roxrud I, et al. SLC9A6 mutations cause X-linked mental retardation, microcephaly, epilepsy, and ataxian, a phenotype mimicking Angelman Syndrome. Am J Hum Genet 2008;82:1003–1010. [PubMed: 18342287]

Glessner JT, Wang K, Cai G, et al. Autism genome-wide copy number variation revelas ubiquitin and neuronal genes. Nature. 2009 advanced online publication.

Greer PL, Greenberg ME. From Synapse to Nucleus: Calcium-Dependent Gene Transcription in the Control of Synapse Development and Function. Neuron 2008;59:846–860. [PubMed: 18817726]

Jiang YH, Armstrong D, Albrecht U, Atkinds CM, Noebels JL, Eichele G, Sweatt JD, Beaudet AL. Mutation of the Angelman ubiquitin ligase in mice causes increased cytoplasmic p53 and deficits of contextual learning and long-term potentiation. Neuron 1998;21:799–811. [PubMed: 9808466]

Kessels HW, Malinow R. Synaptic AMPA receptor plasticity and behavior. Neuron 2009;61:340–350. [PubMed: 19217372]

Kishino T, Lalande M, Wagstaff J. UBE3A/E6-AP mutations cause Angelman Syndrome. Nat Genet 1997;15:70–73. [PubMed: 8988171]

Kumar S, Talis AL, Howley PM. Identification of HHR23A as a substrate for E6-associated protein-mediated ubiquitination. J Biol Chem 1999;274:18785–18792. [PubMed: 10373495]

Lin Y, Bloodgood BL, Hauser JL, Lapan AD, Koon AC, Kim TK, Hu LS, Malik AN, Greenberg ME. Activity-dependent regulation of inhibitory synapse development by Npas4. Nature 2008;455:1198–1204. [PubMed: 18815592]

Man HY, Sekine-Aizawa Y, Huganir RL. Regulation of alpha-amino3-hydroxy-5-methyl-4-isoxazolepropionic acid receptor trafficking through PKA phosphorylation of the Glu receptor 1 subunit. PNAS 2007;104:3579–3584. [PubMed: 17360685]

Matsuura T, Sutcliffe JS, Fang P, Galjaard RJ, Jiang YH, Benton CS, Rommens JM, Beaudet AL. De novo truncating mutations in E6-AP ubiquitin-protein ligase gene (UBE3A) in Angelman Syndrome. Nat Genet 1997;15:74–7. [PubMed: 8988172]

Miura K, Kishino T, Li E, Webber H, Dikkes P, Holmes GL, Wagstaff J. Neurobehavioral and electroencephalographic abnormalities in Ube3A maternaldeficient mice. Neurobiol Dis 2002;9:149–159. [PubMed: 11895368]

Morrow EM, Yoo SY, Flavell SW, Kim TK, Lin Y, Hill RS, Mukaddes NM, Balkhy S, Gascon G, Hasmi A, Al-Saad S, Ware J, Joseph RM, Greenblatt R, Gleason D, Ertelt JA, Apse KA, Bodell A, Partlow JN, Barry B, Yao H, Markianos K, Ferland RJ, Greenberg ME, Walsh CA. Identifying autism loci and genes by tracing recent shared ancestry. Science 2008;321:218–223. [PubMed: 18621663]

Nakamoto M, Nalavadi V, Epstein MP, Naraynan U, Bassell GJ, Warren ST. Fragile X mental retardation protein deficiency leads to excessive mGluR5-dependent internalization of AMPA receptors. Proc Natl Acad Sci 2007;104:15537–15542. [PubMed: 17881561]

Newpher TM, Ehlers MD. Glutamate receptor dynamics in dendritic microdomains. Neuron 2008;58:472–497. [PubMed: 18498731]

Nithianantharajahm J, Hannan AJ. Enriched environments, experience-dependent plasticity and disorders of the nervous system. Nat Rev Neurosci 2006;7:697–709. [PubMed: 16924259]

Oda H, Kumar S, Howley PM. Regulation of the Src family tyrosine kinase BLK through E6AP-mediated ubiquitination. Proc Natl Acad Sci 1999;96:9557–9562. [PubMed: 10449731]

Paradis S, Harrar DB, Lin Y, Koon AC, Hauser JL, Griffith EC, Zhu L, Brass LF, Chen C, Greenberg ME. An RNAi-based approach identifies molecules required for glutamatergic and GABAergic synapse development. Neuron 2007;53:217–232. [PubMed: 17224404]

Park S, Park JM, Kim S, Kim JA, Shepherd JD, Smith-Hicks CL, Chowdhury S, Kaufmann W, Kuhl D, Ryazanov AG, Huganir RL, Linden DJ, Worley PF. Elongation factor 2 and fragile X mental retardation protein control the dynamic translation of Arc/Arg3.1 essential for mGluR-LTD. Neuron 2008;59:70–83. [PubMed: 18614030]

Petrij F, Giles RH, Dauwerse HG, et al. Rubinstein-Taybi syndrome caused by muations in the transcriptional co-activator CBP. Nature 1995;376:348–351. [PubMed: 7630403]

Rial Verde EM, Lee-Osbourne J, Worley PF, Malinow R, Cline HT. Increased expression of the immediate-early gene arc/arg3.1 reduces AMPA receptor-mediated synaptic transmission. Neuron 2006;52:461–474. [PubMed: 17088212]

Rose J, Jin SX, Craig AM. Heterosynaptic molecular dynamics: locally induced propagating synaptic accumulation of CaM kinase II. Neuron 2009;61:351–358. [PubMed: 19217373]

Ryu KY, Maehr R, Gilchrist CA, Long MA, Bouley DM, Mueller B, Ploegh HL, Kopito RR. The mouse polyubiquitin gene UbC is essential for fetal liver development, cell-cycle progression and stress tolerance. EMBO J 2007;26:2693–2706. [PubMed: 17491588]

Scheffner M, Huibregtse JM, Vierstra RD, Howley PM. The HPV-16 E6 and E6-AP complex functions as a ubiquitin-protein ligase in the ubiquitination of p53. Cell 1993;75:495–505. [PubMed: 8221889]

Shepherd JD, Rumbaugh G, Wu J, Chowdhury S, Plath N, Kuhl D, Huganir RL, Worley PF. Arc/Arg3.1 mediates homeostatic synaptic scaling of AMPA receptors. Neuron 2006;52:475–484. [PubMed: 17088213]

Sutcliffe JS, Nurmi EL, Lombroso PJ. Genetics of childhood disorders:XLVII. Autism, part 6: duplication and inherited susceptibility of chromosome 15q11-q13 genes in autism. J Am Acad Child Adoles Psychiatry 2003;42:253–256.

Williams CA, Beaudet AL, Clayton-Smith J, Knoll JH, Kyllerman M, Laan LA, Magenis RE, Moncia A, Schinzel AA, Summers JA, Wagstaff J. Angelman Syndrome 2005: updated consensus for diagnostic criteria. Am J Med Genet A 2006;140:413–418. [PubMed: 16470747]

Van Woerden GM, Harris KD, Hojjati MR, Gustin RM, Qiu S, de Avila Freire R, Jiang YH, Elgersma Y, Weeber EJ. Rescue of neurological deficits in a mouse model for Angelman Syndrome by reduction of alphaCaMKII inhibitory phosphorylation. Nat Neurosci 2007;10:280–282. [PubMed: 17259980]

Yan QJ, Rammal M, Tranfaglia M, Bauchwitz RP. Suppression of two major Fragile X Syndrome mouse model phenotypes by the mGluR5 antagonist MPEP. Neuropharmacology 2005;49:1053–1066. [PubMed: 16054174]

Yashiro K, Riday TT, Condon KH, Roberts AC, Bernardo DR, Prakesh R, Weinberg RJ, Ehlers MD, Philpot BD. Ube3A is required for experience-dependent maturation of the neocortex. Nat Neurosci. 2009 Advanced online publication.

Zhou Z, Hong EJ, Cohen S, Zhao WN, Ho HY, Schmidt L, Chen WG, Lin Y, Savner E, Griffith EC, Hu L, Steen JA, Weitz CJ, Greenberg ME. Brain-specific phosphorylation of MeCP2 regulates activity-dependent Bdnf transcription, dendritic growth, and spine maturation. Neuron 2006;52:255–269. [PubMed: 17046689]

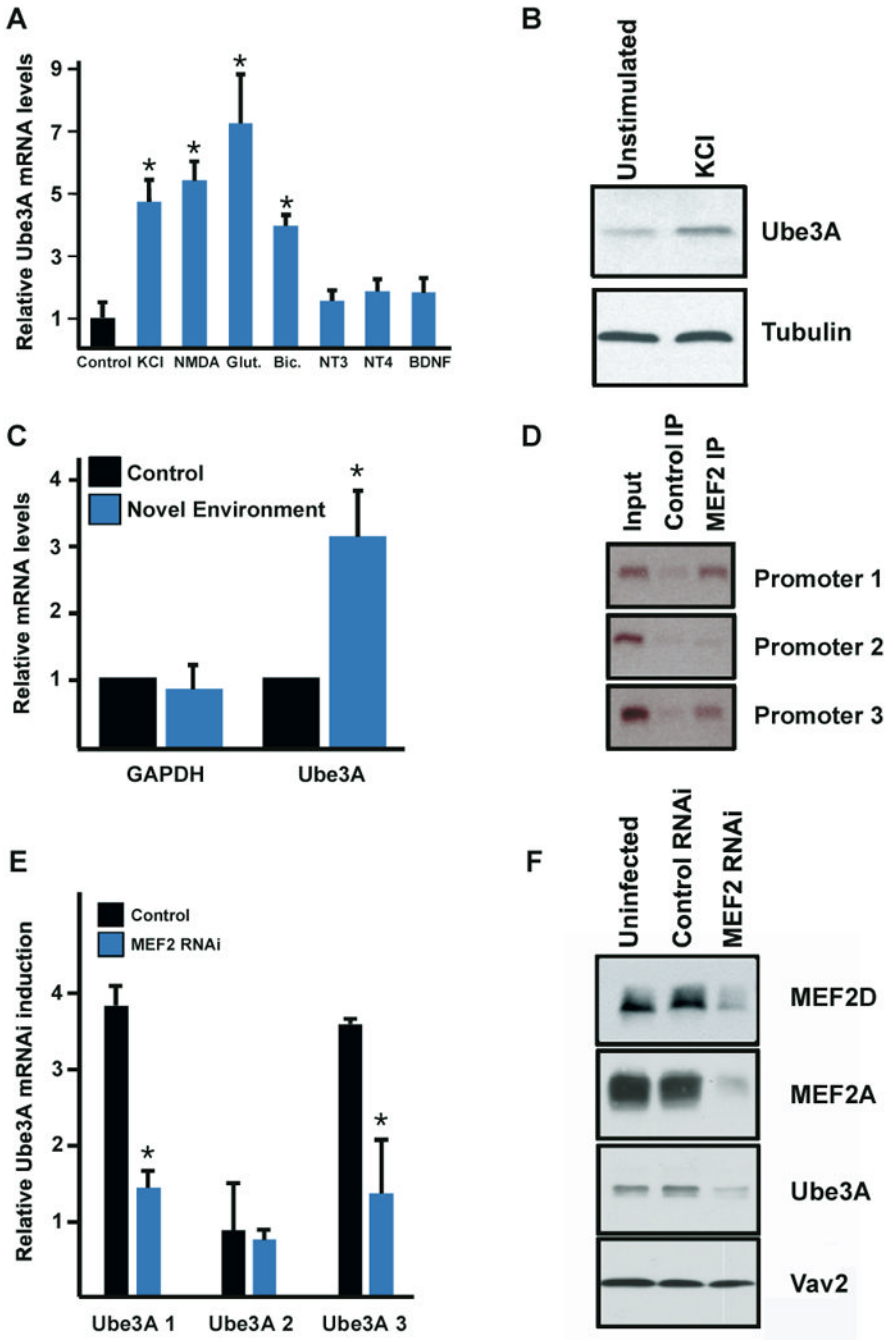

Fig. 1.

Regulation of Ube3A by neuronal activity. (A) qRT-PCR analysis of Ube3A mRNA extracted from hippocampal neurons at E18 + 10 days *in vitro* (DIV) stimulated for five hours with the indicated agent (Glut. = glutamate; Bic. = bicuculline). Data are means +/- SEM from three independent experiments. * indicates statistical significance in pairwise comparison to control: $P < 0.01$ T-test. (B) Western blot analyses of Ube3A and beta-tubulin. Protein lysates were collected from E18 + 10 DIV hippocampal neurons following stimulation with 55 mM KCl for seven hours. Three independent experiments were performed and a representative Western blot is shown. (C) qRT-PCR examining Ube3A and GAPDH mRNA levels in hippocampi of mice placed in standard laboratory cages (control)

or in cages with novel objects (novel environment). The expression of Ube3A and GAPDH is normalized to the expression of beta-tubulin which serves as an internal standard. Data are presented as mean +/- SEM from three independent experiments. * indicates statistical significance in pairwise comparison: $P < 0.05$ T-test. (D) Chromatin immunoprecipitation with control or anti-MEF2 antibodies. PCR amplification is performed on genomic regions corresponding to the promoter regions of the three Ube3A transcripts. (E) qRT-PCR analysis of the three Ube3A transcripts in hippocampal neurons transduced with lentivirus expressing either control shRNA or shRNAs targeting MEF2A and MEF2D. Neurons were stimulated with 55 mM KCl for six hours before mRNA was harvested. Data are plotted as fold induction of stimulated cells over unstimulated cells. Data are presented as mean +/-SEM from three independent experiments. * indicates statistical significance in pairwise comparison: $P < 0.01$ T-test. (F) Western blot analyses of MEF2D, MEF2A, Ube3A, and the loading control Vav2. Protein lysates were collected from hippocampal neurons at E18 + 10 DIV. Neurons were uninfected or transduced with lentivirus encoding a control shRNA or shRNA targeting MEF2A and MEF2D at E18 + 3 DIV. This experiment was performed three times independently and a representative Western blot is shown here. See also Figure S1.

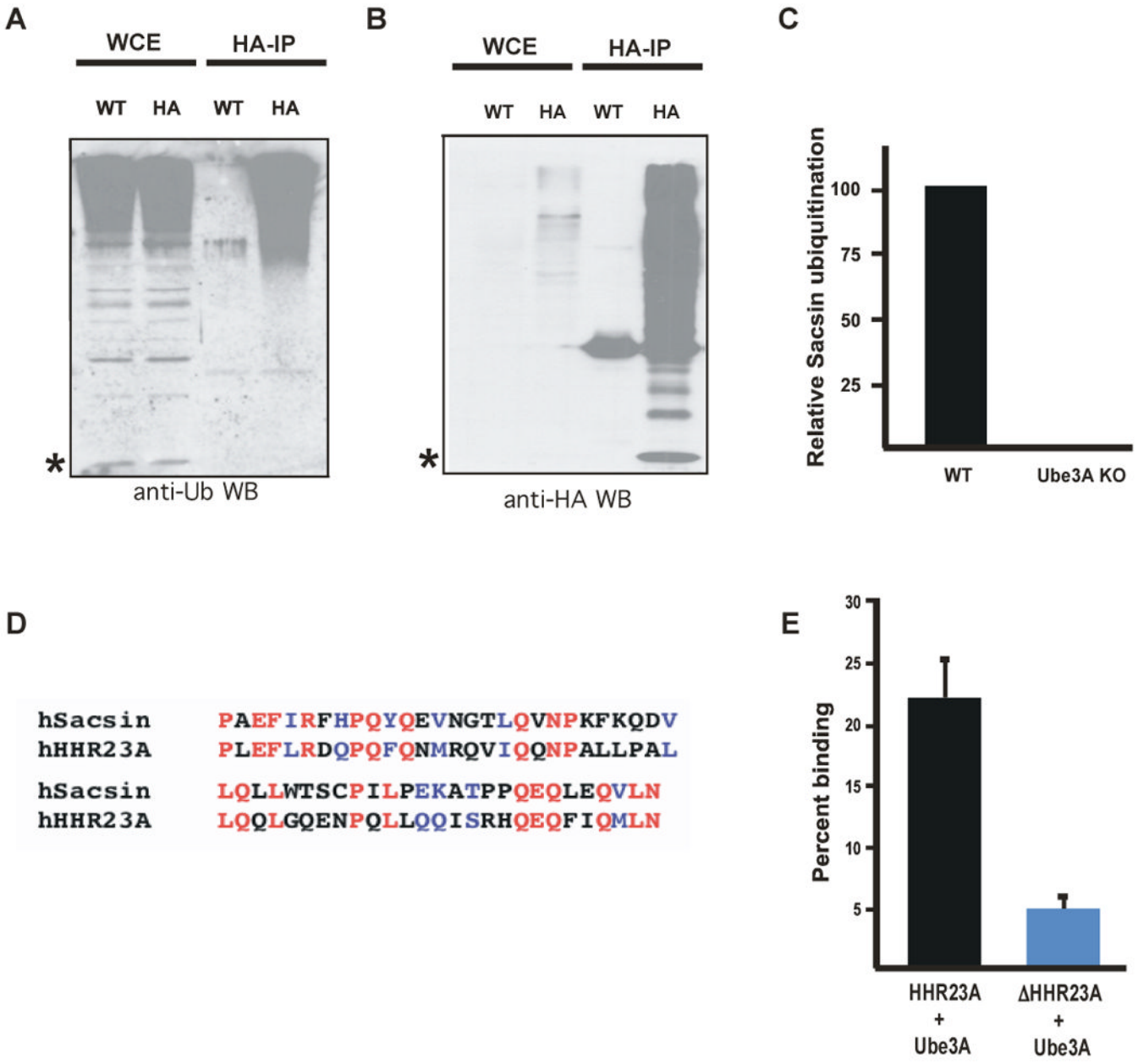

Fig. 2.

Identification of a Ube3A binding domain. (A) Analysis of ubiquitinated proteins in wild type and HA-ubiquitin mice. Western blots using an anti-Ubiquitin antibody were performed on cell lysates (WCE) or anti-HA immunoprecipitates from hippocampal mouse brain lysates prepared from wild type (WT) or HA-ubiquitin transgenice (HA) mice. * indicates the presence of free ubiquitin. (B) Analysis of ubiquitinated proteins in wild type and HA-ubiquitin mice. Western blots using an anti-HA antibody were performed on cell lysates (WCE) or anti-HA immunoprecipitations from hippocampal mouse brain lysates from wild type (WT) or HA-ubiquitin transgenic (HA) mice. * indicates the presence of free ubiquitin. (C) Quantification of the relative abundance of ubiquitinated Sacsin in the brain of wild type and Ube3A knockout mice. No peptides were detected corresponding to ubiquitinated Sacsin in Ube3A knockout mice. (D) Sequence alignment of human Sacsin and human

HHR23A. Identical residues are in red and similar residues are in blue. (E) Quantitative analysis of *in vitro* binding experiments using recombinant HHR23A, a version of HHR23A lacking the Ube3A binding domain (ΔHHR23A), and Ube3A. Western blotting was performed using an anti-HHR23A antibody. Data are presented as mean +/- SEM from three independent experiments.

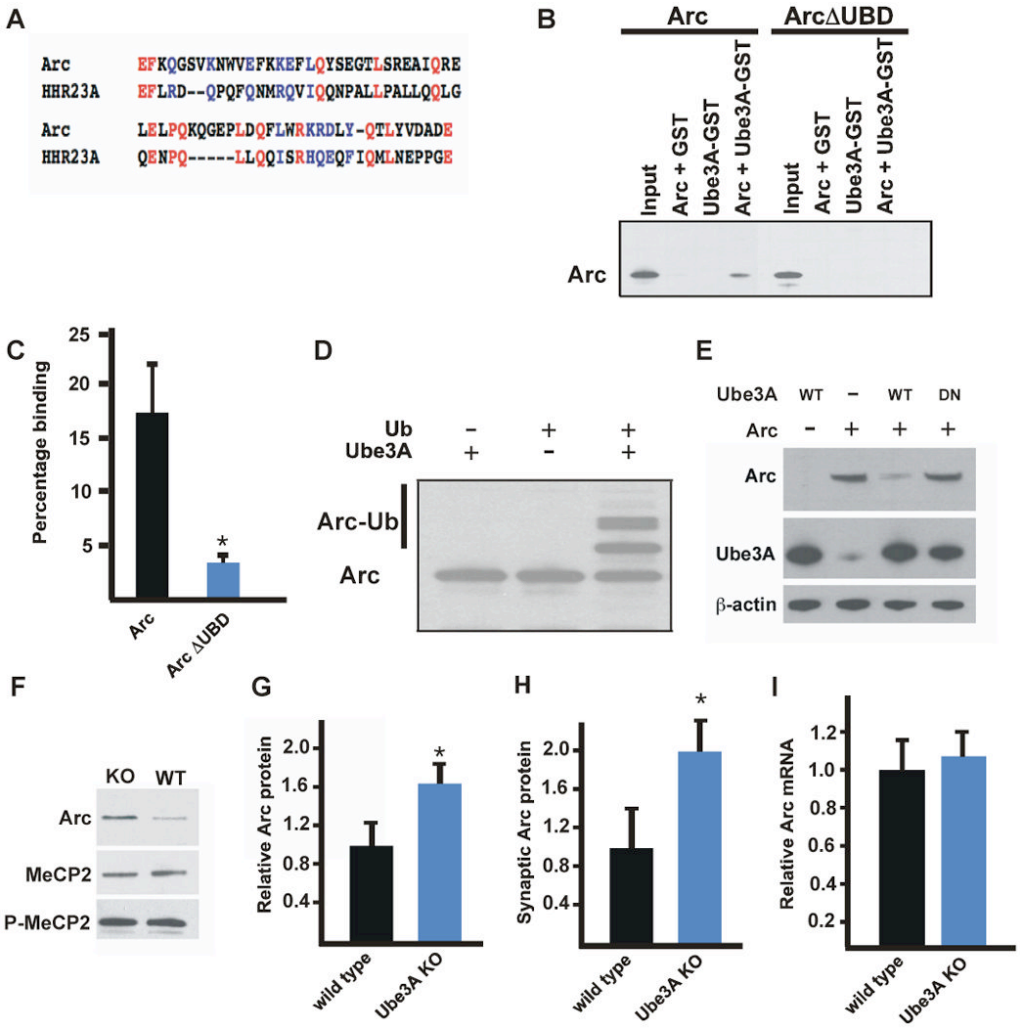

Fig. 3.

Arc is a Ube3A substrate. (A) Sequence alignment of Arc (amino acids 255-318) and HHR23A (amino acids 233-290). Identical residues are in red and similar residues are in blue. We would like to note that as the UBD may represent a sequence that encodes a particular protein folding structure, a strict one-to-one map of specific residues is not observed. (B) *In vitro* binding experiments using recombinant Arc, ArcΔUBD, and GST-tagged Ube3A. (C) Quantitative analysis of *in vitro* binding experiments using recombinant Arc, or ArcΔUBD, and Ube3A. Western blotting was performed using an anti-Arc antibody. Percentage binding refers to the percent of Arc bound to Ube3A relative to the input. Data are presented as mean +/-SEM from three independent experiments. (D) *In vitro* ubiquitination assay of Arc in the presence of Ubiquitin (Ub), and/or Ube3A. (E) Western blot analysis using anti-Arc, anti-Ube3A, or anti-actin antibodies on lysates from HEK293T cells transfected with the indicated constructs. (F) Western blot analysis of protein lysates prepared from the hippocampi of wild type and Ube3A knockout mice which had been injected with kainic acid. Western blots performed with anti-MeCP2, anti-phospho-MeCP2, and anti-Arc antibodies as indicated. Three individual experiments representing at least five animals per genotype were performed and a representative example is shown. (G) Quantification of Arc protein by Western blot analysis of protein lysates prepared from hippocampi of wild type and Ube3A knockout mice which had been exposed to an enriched

environment. Data represent mean +/- SEM from four animals of each genotype. * denotes significance in pairwise comparison to control: $P < 0.01$ T-test. (H) Quantification of Arc protein by Western blot analysis of protein lysates prepared from synaptosomes isolated from hippocampi of wild type and Ube3A knockout mice which had been injected with kainic acid. Data represent mean +/- SEM from three animals of each genotype. * denotes significance in pairwise comparison to control: $P < 0.05$ T-test. (I) Real-time quantitative PCR analysis of Arc mRNA extracted from wild type and Ube3A knockout mice seized with kainic acid used in part (F). Data are presented as mean +/- SEM from three independent experiments. See also Figure S2.

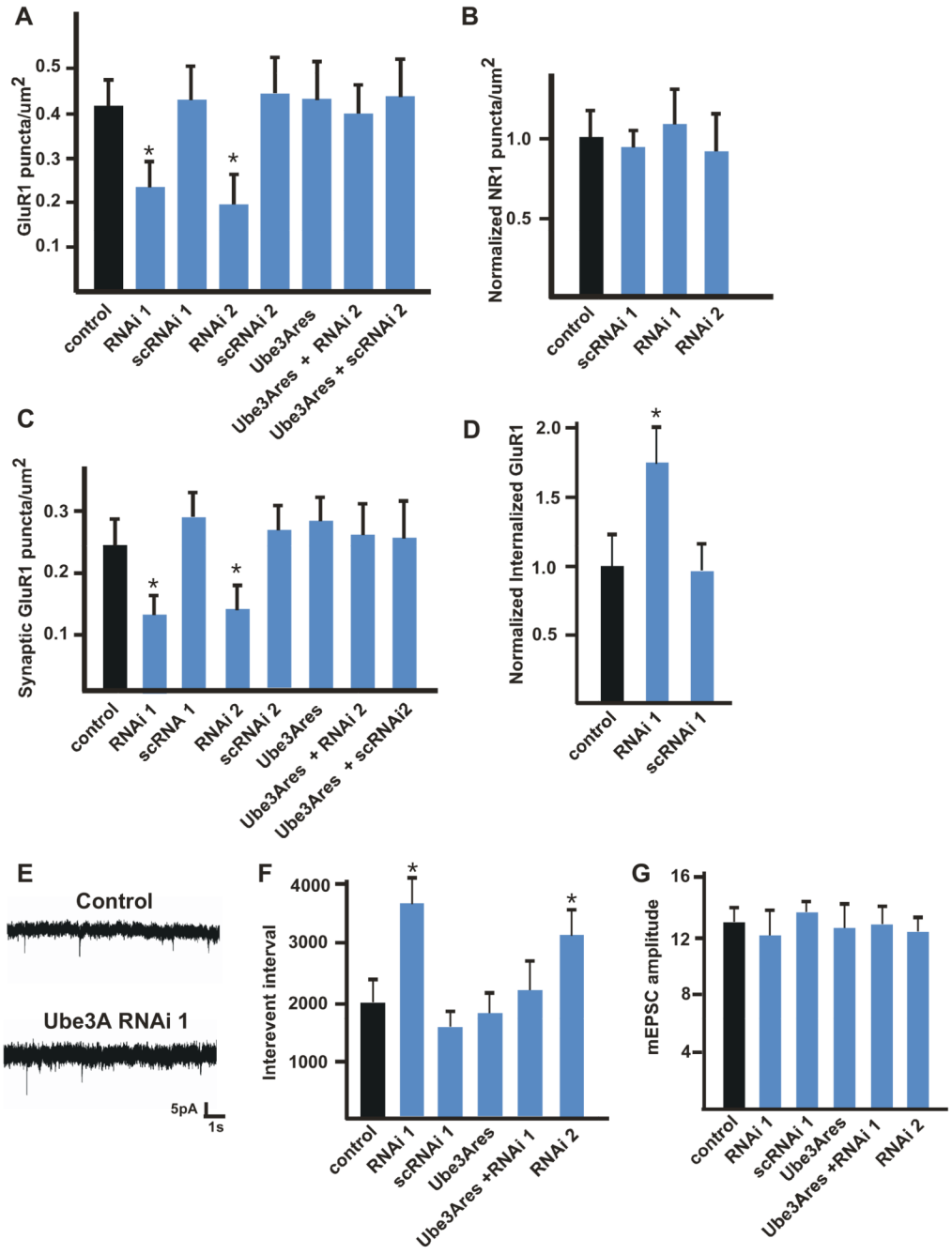

Fig. 4.

Ube3A regulates AMPAR function. (A) Quantification of plasma membrane expression of AMPARs on E18 + 14 DIV hippocampal neurons transfected at 10 DIV with GFP and vector control, either of two shRNAs targeting Ube3A (RNAi 1 or 2), scrambled control shRNA (scRNAi 1 or 2), a form of Ube3A that is resistant to Ube3A shRNA (Ube3Ares) or Ube3A shRNA and Ube3A that is RNAi resistant (Ube3Ares + RNAi 2). At least 35 neurons were imaged for each condition. Data are presented as mean +/- SEM from three independent experiments. * indicates statistical significance $P < 0.05$, ANOVA using a Bonferroni correction for multiple comparisons. (B) Quantification of plasma membrane expression of NMDA receptors on E18 + 14 DIV hippocampal neurons transfected at 10

DIV with GFP and vector control, either of two shRNAs targeting Ube3A (RNAi 1 or 2), or a scrambled control shRNA (scRNAi 1). At least 20 neurons were imaged for each condition, and data are presented as mean +/- SEM from three independent experiments. (C) Same as in (A) except only GluR1 puncta that co-localize with PSD95 are counted. At least 29 neurons were imaged for each condition, and data are presented as mean +/- SEM from three independent experiments. * indicates statistical significance $P < 0.05$, ANOVA using a Bonferroni correction for multiple comparisons. (D) Quantification of internalized GluR1 receptors from E18 + 14 DIV hippocampal neurons transfected at 10 DIV with GFP plus vector, Ube3a shRNA, or control scrambled shRNA. Data are presented as mean +/- SEM from three independent experiments. * indicates statistical significance $P < 0.05$, ANOVA using a Bonferroni correction for multiple comparisons. (E) Representative mEPSC traces of control transfected (top) or Ube3A RNAi transfected neurons (bottom) used for analysis in (F) and (G). (F) Quantification of mEPSC interevent interval (the time between mEPSC events and thus inversely proportional to mEPSC frequency) from E18 + 14 DIV hippocampal neurons transfected as in part (A). Data are presented as mean +/- SEM from three independent experiments. * indicates statistical significance $P < 0.01$, t-test. (G) Quantification of mEPSC amplitude from E18 + 14 DIV hippocampal neurons transfected as in part (A). Data are presented as mean +/- SEM from three independent experiments. See also Figure S3.

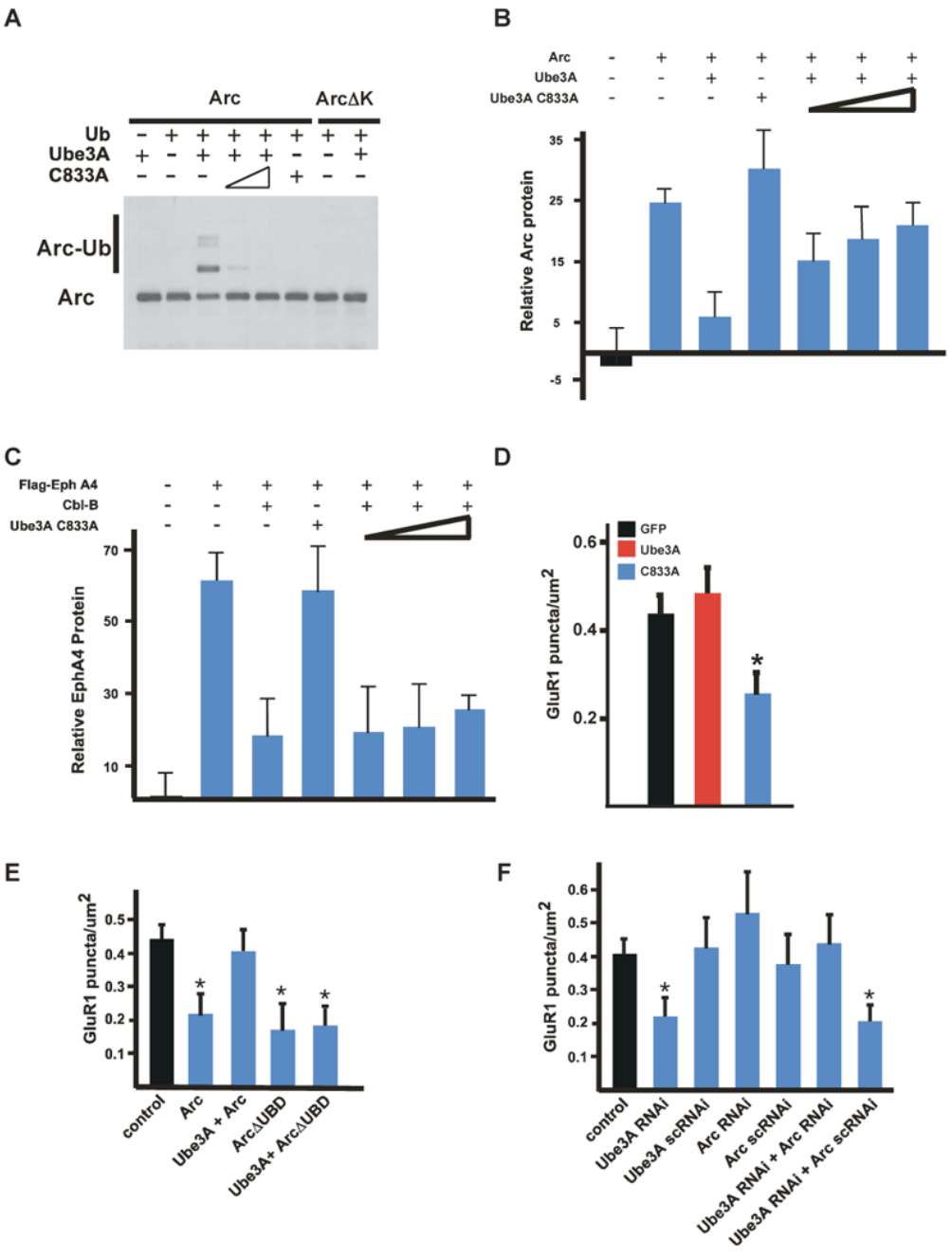

Fig. 5.

Ube3A-mediated degradation of Arc affects AMPAR cell surface expression. (A) *In vitro* ubiquitination assay of Arc or a version of Arc in which all lysine residues are mutated to arginine (ArcΔK) in the presence of Ubiquitin (Ub), Ube3A or Ube3A C833A (C833A). Western blotting analysis was performed with an anti-Arc antibody. (B) Quantitative Western blot analysis of protein lysates from HEK293T cells transfected with the indicated constructs. Western blots were performed using an anti-Arc antibody, and the signals were normalized to an actin loading control. (C) Quantitative Western blot analysis of protein lysates from HEK293T cells transfected with the indicated constructs. Western blots were performed using an anti-Flag antibody to detect EphA4, and the resultant values were

normalized to an actin loading control. As previously reported Cbl-B promotes the degradation of EphA4 (Sharfe et al., 2003). Cbl-B-mediated degradation of EphA4 is not inhibited by Ube3A C833A, even though Ube3A and Cbl-B can employ the same E2 conjugating enzyme when ubiquitinating substrates. (D) Quantification of surface AMPAR expression for E18 + 17 DIV hippocampal neurons transfected with GFP and vector control, Ube3A, or Ube3A C833A plasmids. At least 30 neurons were imaged for each condition and data are presented as mean +/- SEM from three independent experiments. * indicates statistical significance $P < 0.05$, ANOVA, with Bonferroni correction for multiple comparison. (E) Quantification of surface AMPA receptor expression on E18 + 14 DIV hippocampal neurons transfected at 10 DIV with vector control, Arc, Ube3A + Arc, ArcΔUBD, or ArcΔUBD + Ube3A. Data are presented as mean +/- SEM from three independent experiments. * denotes statistical significance $P < 0.05$, ANOVA, with Bonferroni correction for multiple comparison. (F) Quantification of surface AMPAR expression on hippocampal neurons transfected with vector control, Ube3A RNAi, Arc RNAi, Ube3A RNAi and scrambled control Arc RNAi, or Ube3A RNAi and Arc RNAi. Data are presented as mean +/- SEM from three independent experiments. * denotes statistical significance $P < 0.05$, ANOVA, with Bonferroni correction for multiple comparison. See also Figures S4 and S5.

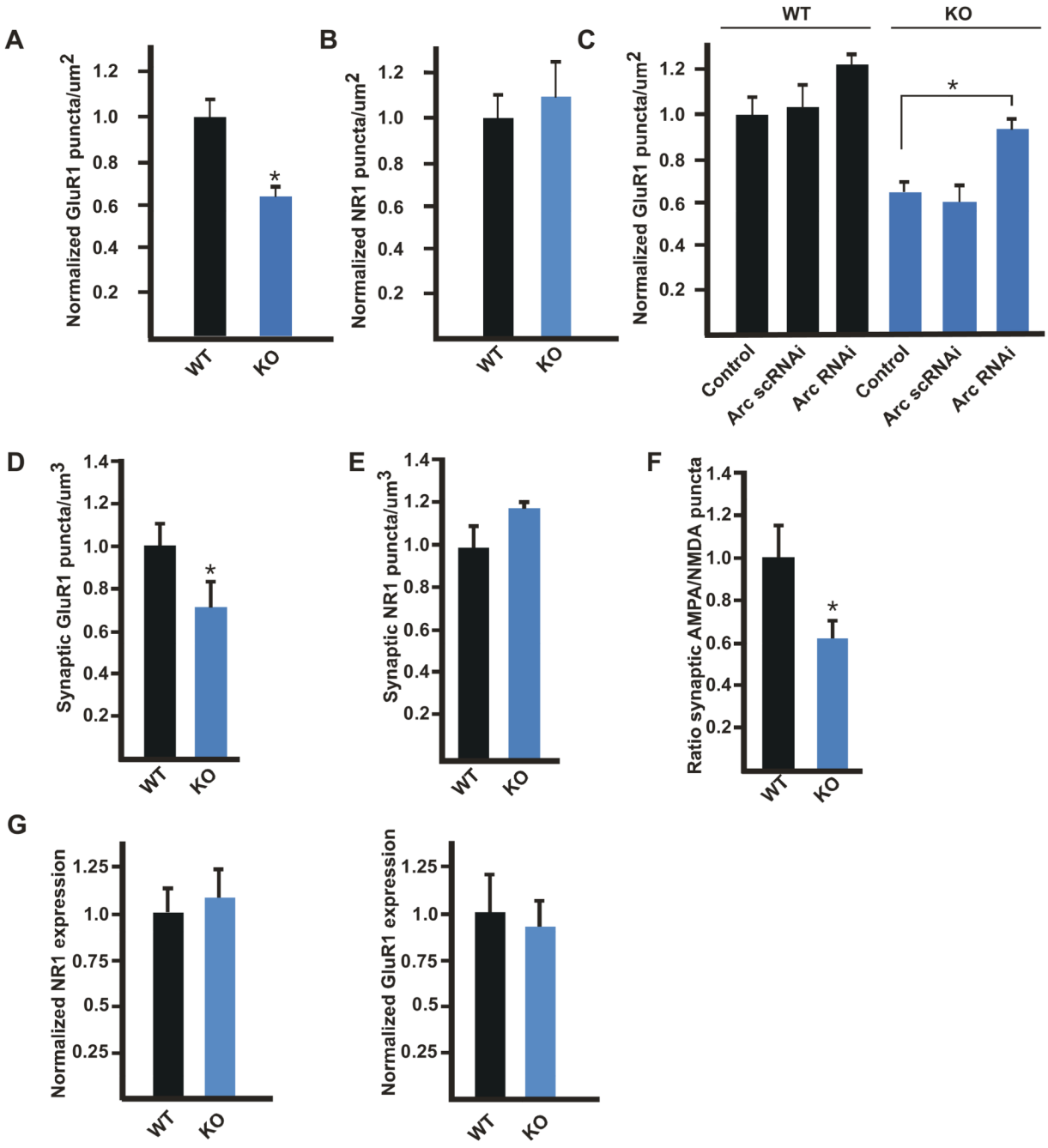

Fig. 6.

Ube3A knockout mice have fewer synaptically expressed AMPARs. (A) Quantification of plasma membrane expression of AMPARs on P2 + 12 DIV hippocampal neurons isolated from wild type (WT) and Ube3A knockout (KO) animals transfected at 8 DIV with GFP. At least 40 neurons were imaged for each condition, and data are normalized to wild type and presented as mean +/- SEM from three independent experiments. * indicates statistical significance $P < 0.01$, T-test. (B) Quantification of plasma membrane expression of NMDA receptors on P2 + 12 DIV hippocampal neurons isolated from wild type (WT) and Ube3A knockout (KO) animals transfected at 8 DIV with GFP. At least 24 neurons were imaged for each condition, and data are normalized to wild type and presented as mean +/- SEM from

three independent experiments. (C) Quantification of plasma membrane expression of AMPA receptors on P2 + 12 DIV hippocampal neurons isolated from wild type (WT) and Ube3A knockout (KO) animals transfected at 8 DIV with GFP and either vector control, scrambled control shRNAs, or shRNAs targeting Arc. At least 28 neurons were imaged for each condition, and data are normalized to wild type transfected with control and presented as mean +/- SEM from three independent experiments. * indicates statistical significance $P < 0.01$, ANOVA, with Bonferroni correction for multiple comparisons. (D) Quantification of the number of co-localized GluR1 and SV2 puncta in wild type and Ube3A knockout hippocampi. Data are presented as mean +/- SEM from three independent animals for each genotype. * indicates statistical significance $P < 0.01$ T-test. (E) Quantification of the number of co-localized NR1 and SV2 puncta in wild type and Ube3A knockout hippocampi. Data are presented as mean +/- SEM from three independent animals for each genotype. $P > 0.05$, T-test. (F) Analysis of the ratio of the density of GluR1 puncta that co-localize with SV2 to the density of NR1 puncta that co-localize with SV2 obtained from (D) and (E). * indicates statistical significance $P < 0.01$ T-test. (G) Quantitative Western blot analysis of protein lysates prepared from the hippocampi of P21 wild type and Ube3A knockout mice using anti-NR1 (left panel) and anti-GluR1 (right panel) antibodies. Band intensity was normalized to the intensity of actin to control for differences in protein concentration. Data are presented as mean +/- SEM from three independent experiments. See also Figure S6.

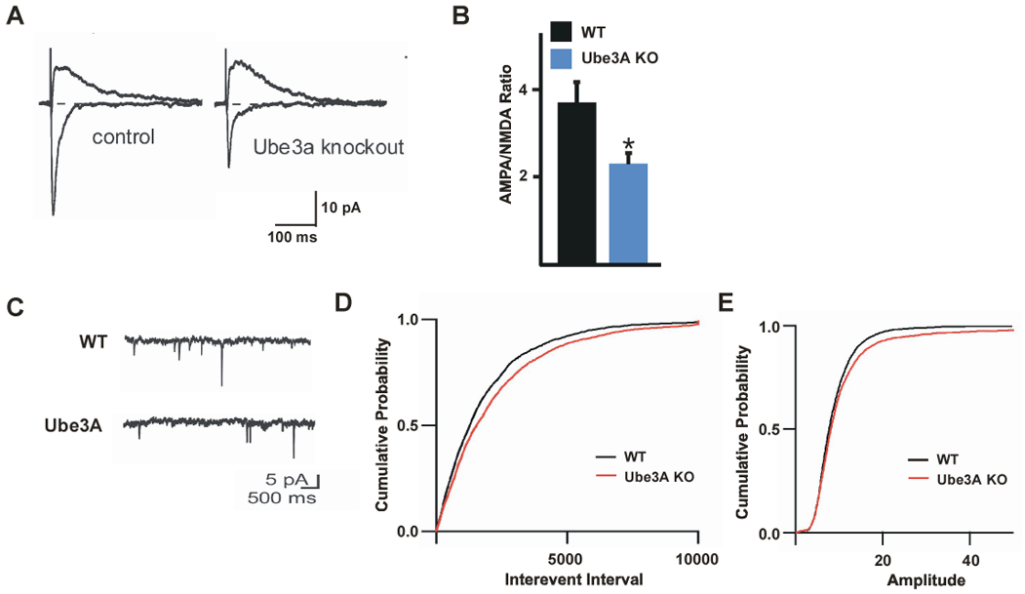

Fig. 7.

Analysis of synaptic function in the hippocampi of Ube3A knockout mice. (A) Representative traces of currents evoked while holding the neuron at -70 or +40 mV to measure AMPAR or NMDAR-mediated currents, respectively. Examples are shown from a control (left) and Ube3A knockout (right) neuron. Currents are scaled by the current amplitude measured between 50 and 70 ms after the peak of the evoked current at +40 mV to highlight the relative changes in AMPAR-mediated current. (B) A summary histogram of AMPA/NMDA receptor-mediated current ratios presented as the geometric mean +/- SEM. At least 15 cells were analyzed per condition. * $p < 0.05$ by students t-test of the geometric means for each neuron. (C) Representative mEPSC traces of hippocampal neurons from wild type (top) and Ube3A knockout neurons (bottom). (D) Quantification of mEPSC frequency from wild type (black line) and Ube3A knockout (red line) mice. Data are presented as cumulative probability plots of interevent intervals and represent recordings from at least 14 neurons from at least three independent animals of each genotype. A significant difference was observed between wild type and Ube3A knockout mice, $P < 0.01$ by KS test. (E) Quantification of mEPSC amplitude from wild type (black line) and Ube3A knockout (red line) mice. Data are presented as cumulative probability plots and represent recordings from at least 14 neurons from at least three independent animals of each genotype. No statistically significant difference was observed between wildtype and Ube3A knockout mice by KS test. See also Figure S7.